

G. MÉCHAIN¹
G. MÉJEAN²
R. ACKERMANN²
P. ROHWETTER³
Y.-B. ANDRÉ¹
J. KASPARIAN², ✉
B. PRADE¹
K. STELMASZCZYK³
J. YU²
E. SALMON²
W. WINN⁴
L.A. (VERN) SCHLIE⁵
A. MYSYROWICZ¹
R. SAUERBREY⁶
L. WÖSTE³
J.-P. WOLF²

Propagation of fs TW laser filaments in adverse atmospheric conditions

¹Teramobile, Laboratoire d'Optique Appliquée, UMR CNRS 7639, ENSTA – Ecole Polytechnique, Centre de l'Yvette, Chemin de la Hunière, 91761 Palaiseau Cedex, France

²Teramobile, LASIM, UMR CNRS 5579, Université Claude Bernard Lyon 1, 43 bd du 11 Novembre 1918, 69622 Villeurbanne Cedex, France

³Teramobile, Institut für Experimentalphysik, Freie Universität Berlin, Arnimallee 14, 14195 Berlin, Germany

⁴Langmuir Laboratory for Atmospheric Research, Geophysical Research Center, New Mexico Institute of Mining and Technology, Socorro, New Mexico, USA

⁵Directed Energy Directorate (AFRL/DELS), Air Force Research Laboratory, 3550 Aberdeen Blvd, SE, Kirtland AFB, NM 87117, USA

⁶Teramobile, Institut für Optik und Quantenelektronik, Friedrich Schiller Universität, Max-Wien-Platz 1, 07743 Jena, Germany

Received: 1 April 2005 / Published online: 9 May 2005 • © Springer-Verlag 2005

ABSTRACT The propagation of femtosecond terawatt laser pulses at reduced pressure (0.7 atm) is investigated experimentally. In such conditions, the non-linear refractive index n_2 is reduced by 30%, resulting in a slightly farther filamentation onset and a reduction of the filament number. However, the filamentation process, especially the filament length, is not qualitatively affected. We also show that drizzle does not prevent the filaments from forming and propagating.

PACS 42.65.Jx; 42.68.Ge; 42.68.-w

1 Introduction

Femtosecond (fs) laser pulses can propagate in air as self-guided filaments [1] as soon as the beam power exceeds a so-called critical power $P_{cr} \sim \lambda^2 / (2\pi n_0 n_2)$ (e.g. $P_{cr} = 3.37\lambda^2 / (8\pi n_0 n_2)$ for a Gaussian beam) [2]. In air, with a refractive index $n_0 \sim 1$ and a non-linear refractive index $n_2 = 3 \times 10^{-23} \text{ m}^2/\text{W}$, $P_{cr} = 3 \text{ GW}$ at a wavelength $\lambda = 800 \text{ nm}$. Under these conditions, Kerr-lens self-focusing overcomes diffraction, so that one or several filaments are formed and propagate with a typical diameter of $100 \mu\text{m}$ over distances much longer than the Rayleigh length, up to several hundreds of meters [3]. Filaments have been observed at distances up to several kilometers [4–6]. The intensity within the filaments is in the order of 10^{14} W/cm^2 [7, 8], allowing self-phase modulation

and generation of a broadband white-light continuum spanning from ultraviolet [9] to the mid infrared [10]. Ionization of the air [11–16] in the filaments crucially contributes to their self-guiding as it allows a dynamic balance with the Kerr effect.

These properties of filaments open exciting perspectives for atmospheric applications [17], such as white-light lidar (light detection and ranging) [4, 18–20], high-voltage discharge switching and guiding or even laser lightning control based on continuous air ionization [21–23], optical telecommunications, or laser-induced breakdown spectroscopy for remote elemental analysis based on the remote delivery of high intensities [24]. Large-scale outdoor applications in turn raise interest for a full characterization of the filament propagation in real atmospheric conditions,

including the low-pressure conditions encountered at high altitudes. The influence of the gas pressure has been investigated on the laboratory scale in several media, especially in rare gases [25–29] and air [30]. Pressure variations induce proportional changes in the group-velocity dispersion (GVD), the non-linear refractive index, and the molecule density available for ionization. Besides this, atmospheric pressure influences the processes of plasma formation and laser–plasma interaction in an essentially non-linear way, mainly by affecting collisional absorption efficiency [31]. On the laboratory scale, pressure mainly affects the relative ionization level, and hence the intensity, within the filaments. However, up to now, little work has been dedicated to the influence of low pressure or pressure gradients [4] at longer scales, although interesting processes like full-beam refocusing have been predicted by some theoretical calculations [32]. Besides effects of reduced pressure, a realistic model for the real-scale propagation of filaments in the atmosphere must take into account the influence of water droplets (i.e. haze, clouds, or rain) on the non-linear propagation of high-power laser pulses. It has recently been shown that single [33–35] and multiple [36] filaments can survive their interaction with dense clouds or fog. However, the possibility of initiating filaments in the

✉ Fax: +33-472445871, E-mail: jkaspari@lasim.univ-lyon1.fr

rain itself, rather than propagating pre-formed filaments in a subsequent cloud, has never been demonstrated to date. Moreover, previous experiments have been performed on synthetic rain, which could result in a biased droplet-size distribution.

In this paper, we characterize the multifilamenting propagation of a fs terawatt (TW) laser beam in adverse conditions at high altitude. In particular, we show that the reduced pressure reduces the filament number without qualitatively affecting the filamentation process, and that filaments can actually be generated and propagated in natural rain.

2 Experimental setup

The laser source used in the experiments was the *Teramobile* mobile femtosecond terawatt laser system [37]. This system allows outdoor experiments under virtually any atmospheric conditions, as was required for measurements over an extended period of two months under various meteorological conditions at a high-altitude location. The *Teramobile* delivers 280-mJ pulses centered at 800 nm, with a repetition rate of 10 Hz. The beam is emitted parallel or slightly focused, with an initial beam diameter of 3 cm. The minimum pulse duration was 150 fs, although a chirp can be applied to the pulses in order to precompensate for GVD in air, resulting in initial pulse durations up to 1.5 ps. In that case, the pulses are refocused temporarily by GVD after a given propagation distance [38].

The *Teramobile* beam was propagated horizontally over 325 m on the Magdalena Mountain ridge (New Mexico, 3230-m altitude above sea level). The standard pressure at this altitude is 0.67 atm, i.e. 6.8×10^4 Pa. The laser beam propagation was characterized by recording beam profiles. They were acquired by taking photographs of the beam on a screen using a digital camera. The exposure time of 1/8 s was chosen to assure that each picture corresponds to a single-shot picture. Images have been taken over both the whole spectrum, with high sensitivity to the white-light continuum and to the conical emission, and in the infrared (fundamental) region of the spectrum, yielding a good approximation of the beam profile

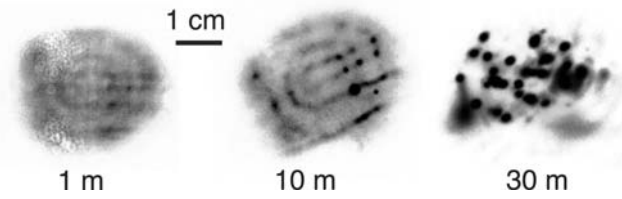


FIGURE 1 Grey-scale intensity profiles of the laser beam on a screen for three propagation distances

at the considered distance, as demonstrated in Ref. [39]. The occurrence of filaments at a given distance was also characterized by single-shot burns on impact paper (Kodak Linagraph, 1895). The darkening of the photosensitive paper yields the intensity profile, while ablation craters in the center of a hot spot characterize a plasma string.

3 Results and discussion

3.1 Propagation at reduced pressure

Figure 1 shows beam profiles after propagation over 1 to 30 m. These profiles are qualitatively similar to equivalent profiles acquired at sea level [6, 39]. More specifically, high-intensity ‘fork’ structures appear within the beam profile, and filaments are later generated on these intensity ridges.

The position of the filament onset (z_f) provides a good characterization of the first phase of filamentation, namely the self-focusing (Kerr) region. It is given by the Marburger formula [2]

$$\frac{1}{z_f(P)} = -\frac{1}{R} \pm \frac{\sqrt{(\sqrt{P/P_{\text{crit}}} - 0.852)^2 - 0.0219}}{0.367ka^2}, \quad (1)$$

where R is the initial wavefront curvature (in our case, $R = f \sim 50$ m), P is the laser power, k is the wave number, and a is the radius of the beam, defined as the half width at $e^{-1/2}$.

In the self-focusing region, the propagation is governed by Kerr self-focusing and hence by the non-linear refractive index n_2 of the air, which is proportional to the pressure [40]. Therefore, the critical power is inversely proportional to the air pressure, and z_f is strongly affected in the low-power regime, when $P \sim P_{\text{cr}}$. However, the asymptotic behavior of Eq. (1) for high powers ($P \gg P_{\text{cr}}$) leads to a square-root pressure dependence so that, in our experiment, a 30% reduction in the atmospheric pressure only results in 15% shortening of z_f . Such an estimation cannot be compared with the experimental data (see Fig. 2), due to the limited range resolution (5 m). However, the reduced pressure does not significantly affect the filamentation length. The length observed in Fig. 2 is comparable with measurements performed under similar conditions close to sea level (155-m altitude), suggesting that the loss due to the multiphoton ionization of air is not significantly different from its value at sea level. [6]

Another key parameter is the number of filaments. A multifilamenting beam breaks up into cells containing several

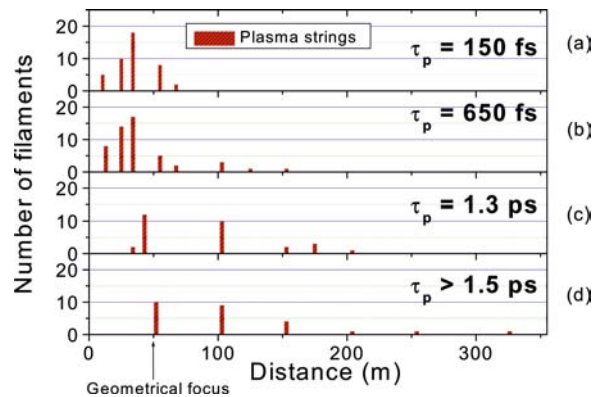


FIGURE 2 Filamentation range for 280-mJ pulses, with an initial pulse duration of **a** $\tau_p = 150$ fs, **b** $\tau_p = 650$ fs, **c** $\tau_p \sim 1.3$ ps, and **d** $\tau_p \sim 1.5$ ps

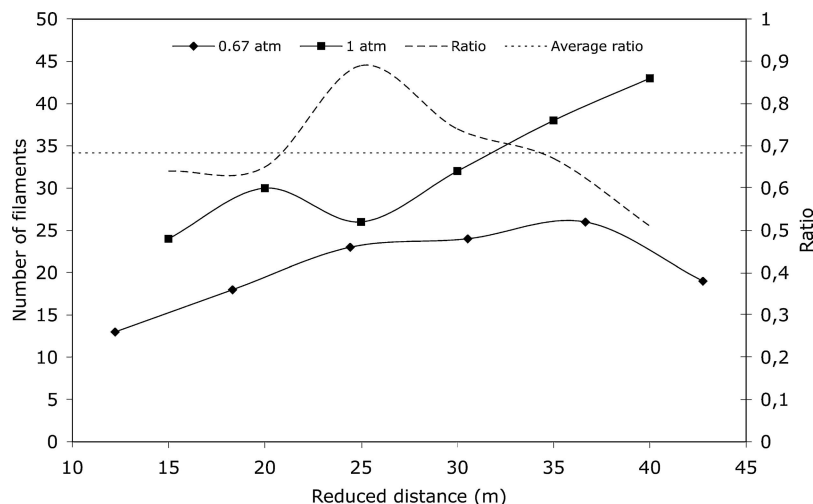


FIGURE 3 Comparison of the filament number generated by 2.5-TW pulses at 0.67 atm (3200-m altitude) and 1 atm (sea level) for corresponding reduced propagation distances (*left-hand scale*). The ratio of the filament numbers in both conditions is plotted relative to the *right-hand scale*. See the text for the definition of reduced distances

(typically 1 to 10) critical powers [36]. Hence, the number of filaments is inversely proportional to P_{cr} , and therefore proportional to the pressure. Figure 3 correlates the filament numbers observed at 0.67-atm air pressure with those observed under similar conditions (2.5 TW, 150 fs) at sea level (Lyon, France, 170-m altitude) [36], for several propagation distances. Here, filaments have been identified as localized, high-intensity hot spots in the beam profiles. To compare filament numbers at similar stages of filamentation, the data are plotted as a function of the reduced propagation distance $\hat{z} = z/\sqrt{p/p_0} = z z_f/z_f(p_0)$, where z is the propagation distance and p the atmospheric pressure, and the 0 subscript corresponds to the standard atmospheric pressure. The square root of p stems from the asymptotic behavior of Eq. (1). A fairly good proportionality is observed between the filament numbers at 1 and 0.67 atm, and the average reduction of the filament number (32%) corresponds to the pressure reduction and hence to the drop in the critical power. It indeed shows that the beam breaks up into cells containing some P_{cr} each [36].

We further investigated the influence of power on the filament number by varying the chirp and observing the beam profile on photographic paper [6]. Figure 2 displays the number of plasma strings (filaments) as a function of the propagation distance for various pulse durations. The lower peak power of

longer pulses results in a farther filamentation onset (i.e. closer to the geometrical focus, $z \sim 50$ m). A stronger chirp also results in fewer plasma channels, but over a longer filamentation range. Filaments could be observed up to 325-m distance for chirps corresponding to ~ 1.5 – 1.8 -ps pulse length.

The present observation of filamentation at a high altitude confirms a recent observation of filamentation in air at pressures as low as 0.2 atm, corresponding to an altitude over 11 km [30]. Moreover, our results extend this observation to the high-power, multifilamentation regime over several hundreds of meters. The fact that the filaments themselves are not qualitatively affected shows that the expected slightly lower free electron density in the plasma channels, due to the lower air-molecule density, does not have a significant effect.

3.2 Filament generation in rain

Besides reduced pressure at high altitudes, the filamentation under real atmospheric conditions includes the propagation in water clouds and rain. The interaction of a fs TW laser beam with rain was investigated by propagating the strongly chirped Teramobile beam over 150 m in drizzle consisting of small (< 0.5 mm) droplets with a rain flow of several mm per hour. The estimated visibility was 150 m, i.e. an extinction coefficient of 6.6 km^{-1} or 37% transmission over 150 m. In the cloud, the estimated droplet density is $1.7 \times 10^4 \text{ m}^{-3}$ so that the 3-cm beam hits approximately one droplet for every cm propagation. Contrary to previous experiments [33, 36], where previously formed filaments interacted with a synthetic cloud, in the present experiment the whole beam interacted with water droplets, even before the filaments were initiated.

Figure 4 compares impacts on photosensitive paper at 75-m distance with and without rain. Filaments are clearly identified as intense spots on the impact paper, with ablation of the paper in their center. This provides evidence for the ability of the filaments to form in rain. The comparison between both images shows that filamentation was not perturbed by the rain, even at reduced pressure, i.e. under conditions of weaker Kerr effect. Further propagation of the filamentation process in rain was also observed up to 150 m (Fig. 5).

Therefore, rain does not prevent the filaments from being generated in the propagation of ultra-short, high-power laser pulses. Since the beam used in our experiments is much above the critical power, the losses induced by the

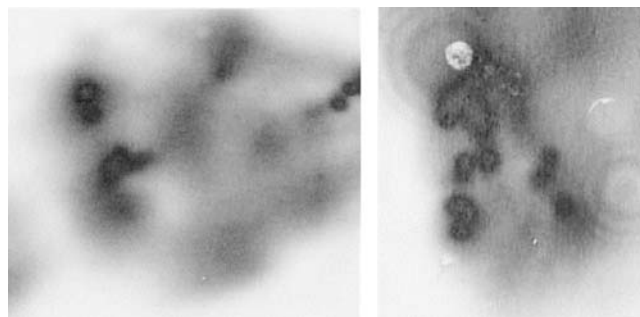


FIGURE 4 Single-shot beam impacts on photosensitive papers after 75-m propagation in dry air (*left*) and in rain (*right*). The air pressure is 0.67 atm (altitude 3230 m). Filaments are clearly visible in both cases. The ring patterns on the profile in rain are due to the diffraction of the beam on the rain droplets

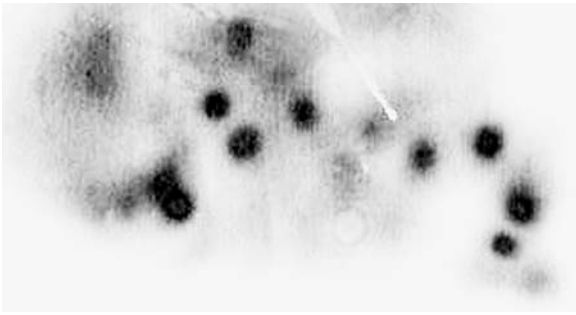


FIGURE 5 Beam impacts on photosensitive paper after 150-m propagation in rain

scattering on the water droplets in the self-focusing (prefilamentation) region are not sufficient to prevent the self-focusing process. Moreover, one can expect that diffraction on water droplets deforms the beam profile and could generate local transverse intensity gradients. Since the self-focusing action of the Kerr effect is due to such gradients, the local intensity dips caused by the droplets could even provide nucleation centers for self-focusing and filamentation. Our observation shows that this possible positive contribution to filamentation roughly balances that of the power losses by diffraction. Once the filamentation is established, the survival of the filaments can be understood by the continuous feeding by the photon bath, as on the laboratory scale [33–35]. Filaments can therefore form and propagate in spite of rain.

4 Conclusion

As a conclusion, we have presented the first experimental data about the propagation of high-power ultrashort laser pulses at reduced pressure over atmospheric scale distances. Lower pressures result in fewer filaments forming at longer distances, but without qualitatively affecting the filamentation process. Moreover, the reduced Kerr effect at high altitude does not prevent filamentation from being initiated and propagating in natural rain. The limited perturbation of both altitude and rain on filamentation is favorable for real-scale applications, which require actual filamentation at remote distances and/or high altitudes or vertical propagation in the case of atmospheric profiling, in clear atmosphere as well as under adverse weather.

ACKNOWLEDGEMENTS This work has been performed within the framework of the *Teramobile* collaboration, funded jointly by the CNRS, DFG, and French and German Ministries

of Foreign Affairs. The authors also acknowledge AFOSR and AFRL/DE for their financial support of the experimental campaign. K.S. acknowledges financial support by the Alexander von Humboldt Foundation. We would like to warmly thank the team of the Langmuir Laboratory at the New Mexico Institute of Mining and Technology, and especially Graydon Aulich, Gary Coppler, James Dinallo, Steven Hunyady, Sandy Kieft, Dan Klinglesmith, William Rison, and William Winn for their constant support all along the campaign. The efficient administrative support by Anne Gourlan at Lasim was also highly appreciated. The *Teramobile* web site is www.teramobile.org.

REFERENCES

- 1 A. Braun, G. Korn, X. Liu, D. Du, J. Squier, G. Mourou, *Opt. Lett.* **20**, 73 (1995)
- 2 J.H. Marburger, E.L. Dawes, *Phys. Rev. Lett.* **21**, 556 (1968)
- 3 B. La Fontaine, F. Vidal, Z. Jiang, C.Y. Chien, D. Comtois, A. Desparois, T.W. Johnston, J.-C. Kieffer, H. Pépin, *Phys. Plasmas* **6**, 1615 (1999)
- 4 M. Rodriguez, R. Bourayou, G. Méjean, J. Kasparian, J. Yu, E. Salmon, A. Scholz, B. Stecklum, J. Eislöffel, U. Laux, A.P. Hatzes, R. Sauerbrey, L. Wöste, J.-P. Wolf, *Phys. Rev. E* **69**, 036607 (2004)
- 5 G. Méchain, A. Couairon, Y.-B. André, C. D'Amico, M. Franco, B. Prade, S. Tzortzakis, A. Mysyrowicz, R. Sauerbrey, *Appl. Phys. B* **79**, 379 (2004)
- 6 G. Méchain, C. D'Amico, Y.-B. André, S. Tzortzakis, M. Franco, B. Prade, A. Mysyrowicz, A. Couairon, E. Salmon, R. Sauerbrey, *Opt. Commun.* **247**, 171 (2005)
- 7 J. Kasparian, R. Sauerbrey, S.L. Chin, *Appl. Phys. B* **71**, 877 (2000)
- 8 A. Becker, N. Aközbe, K. Vijayalakshmi, E. Oral, C.M. Bowden, S.L. Chin, *Appl. Phys. B* **73**, 287 (2001)
- 9 N. Aközbe, A. Iwasaki, A. Becker, M. Scalora, S.L. Chin, C.M. Bowden, *Phys. Rev. Lett.* **89**, 143901 (2002)
- 10 J. Kasparian, R. Sauerbrey, D. Mondelain, S. Niedermeier, J. Yu, J.-P. Wolf, Y.-B. André, M. Franco, B. Prade, A. Mysyrowicz, S. Tzortzakis, M. Rodriguez, H. Wille, L. Wöste, *Opt. Lett.* **25**, 1397 (2000)
- 11 H. Schillinger, R. Sauerbrey, *Appl. Phys. B* **68**, 753 (1999)
- 12 S. Tzortzakis, B. Prade, M. Franco, A. Mysyrowicz, *Opt. Commun.* **181**, 123 (2000)
- 13 B. La Fontaine, F. Vidal, Z. Jiang, C.Y. Chien, D. Comtois, A. Desparois, T.W. Johnston, J.-C. Kieffer, H. Pépin, H.P. Mercure, *Phys. Plasmas* **6**, 1615 (1999)
- 14 A. Talebpour, A. Abdel-Fattah, S.L. Chin, *Opt. Commun.* **183**, 479 (2000)
- 15 J. Kasparian, R. Sauerbrey, S.L. Chin, *Appl. Phys. B* **71**, 877 (2000)
- 16 A. Talebpour, J. Yang, S.L. Chin, *Opt. Commun.* **163**, 29 (1999)
- 17 J. Kasparian, M. Rodriguez, G. Méjean, J. Yu, E. Salmon, H. Wille, R. Bourayou, S. Frey, Y.-B. André, A. Mysyrowicz, R. Sauerbrey, J.-P. Wolf, L. Wöste, *Science* **301**, 61 (2003)
- 18 P. Rairoux, H. Schillinger, S. Niedermeier, M. Rodriguez, F. Ronneberger, R. Sauerbrey, B. Stein, D. Waite, C. Wedekind, H. Wille, L. Wöste, *Appl. Phys. B* **71**, 573 (2000)
- 19 G. Méjean, J. Kasparian, E. Salmon, J. Yu, J.-P. Wolf, R. Bourayou, R. Sauerbrey, M. Rodriguez, L. Wöste, H. Lehmann, B. Stecklum, U. Laux, J. Eislöffel, A. Scholz, A.P. Hatzes, *Appl. Phys. B* **77**, 357 (2003)
- 20 G. Méjean, J. Kasparian, J. Yu, S. Frey, E. Salmon, J.-P. Wolf, *Appl. Phys. B* **78**, 535 (2004)
- 21 B. La Fontaine, D. Comtois, C.Y. Chien, A. Desparois, F. Gérin, G. Jarry, T.W. Johnston, J.C. Kieffer, F. Martin, R. Mawassi, H. Pépin, F.A.M. Rizk, F. Vidal, C. Potvin, P. Couture, H.P. Mercure, *J. Appl. Phys.* **88**, 610 (2000)
- 22 M. Rodriguez, R. Sauerbrey, H. Wille, L. Wöste, T. Fujii, Y.-B. André, A. Mysyrowicz, L. Klingbeil, K. Rethmeier, W. Kalkner, J. Kasparian, E. Salmon, J. Yu, J.-P. Wolf, *Opt. Lett.* **27**, 772 (2002)
- 23 R. Ackermann, K. Stelmaszczyk, P. Rohwetter, G. Méjean, E. Salmon, J. Yu, J. Kasparian, G. Méchain, V. Bergmann, S. Schaper, B. Weise, T. Kumm, K. Rethmeier, W. Kalkner, J.P. Wolf, L. Wöste, *Appl. Phys. Lett.* **85**, 5781 (2004)
- 24 K. Stelmaszczyk, P. Rohwetter, G. Méjean, J. Yu, E. Salmon, J. Kasparian, R. Ackermann, J.-P. Wolf, L. Wöste, *Appl. Phys. Lett.* **85**, 3977 (2004)
- 25 M. Mlejnek, E.M. Wright, J.V. Moloney, *Phys. Rev. E* **58**, 4903 (1998)
- 26 S. Champeaux, L. Bergé, *Phys. Rev. E* **68**, 066603 (2003)
- 27 A. Becker, N. Aközbe, K. Vijayalakshmi, E. Oral, C.M. Bowden, S.L. Chin, *Appl. Phys. B* **73**, 287 (2001)
- 28 N. Kortsalioudakis, M. Tatarakis, N. Vakakis, S.D. Moustazis, S. Tzortzakis, M. Franco, B. Prade, A. Mysyrowicz, N. Papadogiannis, A. Couairon, *Appl. Phys. B* **80**, 211 (2005)
- 29 C.P. Hauri, W. Kornelis, F.W. Helbing, A. Couairon, A. Mysyrowicz, J. Biegert, U. Keller, *Appl. Phys. B* **79**, 673 (2004)
- 30 G. Méchain, T. Olivier, M. Franco, A. Couairon, B. Prade, A. Mysyrowicz, Femtosecond filamentation in air at low pressure, part II: laboratory experiments in preparation
- 31 P. Chylek, M.A. Jarzembki, V. Srivastava, R.G. Pinnick, *Appl. Opt.* **29**, 2303 (1990)
- 32 P. Sprangle, J.R. Peñano, B. Hafizi, *Phys. Rev. E* **66**, 046418 (2002)
- 33 F. Courvoisier, V. Boutou, J. Kasparian, E. Salmon, G. Méjean, J. Yu, J.-P. Wolf, *Appl. Phys. Lett.* **83**, 213 (2003)
- 34 M. Kolesik, J.V. Moloney, *Opt. Lett.* **29**, 590 (2004)

- 35 S. Skupin, L. Bergé, U. Peschel, F. Lederer, Phys. Rev. Lett. **93**, 023901 (2004)
- 36 G. Méjean, J. Kasparian, J. Yu, E. Salmon, S. Frey, J.-P. Wolf, S. Skupin, A. Vinçotte, R. Nuter, S. Champeaux, L. Bergé, submitted to Phys. Rev. E
- 37 H. Wille, M. Rodriguez, J. Kasparian, D. Mondelain, J. Yu, A. Mysyrowicz, R. Sauerbrey, J.P. Wolf, L. Wöste, Eur. Phys. J. – Appl. Phys. **20**, 183 (2002)
- 38 J. Kasparian, J.-P. Wolf, Opt. Commun. **152**, 355 (1998)
- 39 L. Bergé, S. Skupin, F. Lederer, G. Méjean, J. Yu, J. Kasparian, E. Salmon, J.P. Wolf, M. Rodriguez, L. Wöste, R. Bourayou, R. Sauerbrey, Phys. Rev. Lett. **92**, 225 002 (2004)
- 40 E.R. Peck, J.D. Fischer, J. Opt. Soc. Am. **54**, 1362 (1964)